Chinese Journal of Chemical Engineering 53 (2023) 63–72

Contents lists available at ScienceDirect

Chinese Journal of Chemical Engineering

journal homepage: www.elsevier.com/locate/CJChE

Full Length Article

Investigation on catalytic distillation for ethyl acetate production with different catalytic packing structures

Zhiwei Wang, Yu Zhang, Zhi Zhang, Daowei Zhou, Zhikai Cao, Yong Sha *

Department of Chemical and Biochemical Engineering, College of Chemistry and Chemical Engineering, Xiamen University, Xiamen 361005, China

ARTICLE INFO

Article history:
Received 9 December 2021
Received in revised form 12 February 2022
Accepted 24 February 2022
Available online 03 March 2022

Keywords:
Catalytic packing
Ethyl acetate
Catalytic distillation
Mass transfer
Esterification
Reaction kinetics

ABSTRACT

The catalytic packing is the core component of the catalytic distillation, and how the catalyst exists in the packing has significant influence on the process. To investigate the effect of catalyst packings on the catalytic distillation process, the classical ethyl acetate reactive distillation system was utilized, and a supported catalytic packing (SCP) was prepared in comparison with the conventional tea-bag catalytic packing (TBP). Laboratory scale experiments showed that the ethyl acetate conversion of the SCP was superior to the TBP at a low catalyst loading. The effects of reaction kinetics, mass transfer performance and actual catalytic efficiency of the packings on this process were regarded as reasons and studied by combining the experiments and numerical simulation. Results suggested that the relatively immediate "*in-situ* separation" caused by the rapid reaction kinetics and better mass transfer performance of SCP may be a main reason for the difference of the conversion.

1. Introduction

The catalytic distillation (CD) process combines chemical reaction and distillation into one device, and it can significantly reduce investments and energy consumption [1]. The catalytic packing, as one of the key hardware in the CD columns, is widely utilized to ensure the reaction and separation of the CD process [2]. The existence form of the catalyst in the catalytic packing has significant influence on the performance of the CD process due to the coupled reaction-mass transfer process happening in the catalytic packing [3,4]. Better packing design can maximize the synergy of reaction and mass transfer to achieve higher conversion in the CD.

Nowadays, the conventional catalytic packing takes the form of "sandwich" or "tea bag", and the solid acid particle catalysts are fixed in the wire mesh or the binding bag which can ensure a large loading amount [5]. However, this existence form of the catalyst also causes a big diffusion resistance inside the "sandwich" or "tea bag" due to stacked catalyst particles [6]. Therefore, improvement to the transfer performance of these conventional catalytic packings has always been a point of interest in this field.

Through optimizing the geometry of the catalytic packing by means of the computational fluid dynamics, many studies [7–9] were carried out to improve the macroscopic hydrodynamics performance of the catalytic packing while influence of the interaction between the multi component mass transfer and chemical reaction among catalyst particles on the process was ignored. However, results from works, such as Wang *et al.* [10], showed that for the catalytic packing like the tea bag bundle in the hydrolysis process of methyl acetate, the efficiency factor of the tea bag bundle can be increased to 200% when the equivalent diameter of the tea bag was reduced from 25.4 to 8.1 mm. Obviously, change of the structure or geometry of the catalytic packing influences the catalytic reaction and mass transfer simultaneously in the catalytic packing. Therefore, a common means in industry to improve performance of a CD column is to optimize its catalyst loading form. Such as Katapak-SP11 and Katapak-SP12 manufactured by Sulzer [11], the proportion of the separation and reaction module is designed specifically according to process requirements. The percolation catalytic packing was also be utilized to enhance the transfer performance by Li *et al.* [12] and Gao *et al.* [13]. Their experiments showed that percolation through the packing can result in a positive effect on the process, and change of the mass transfer inside the catalytic packing had significant influence on the coupled reaction–separation CD process.

To decrease mass transfer resistance due to stacked catalyst particles inside the packing such as sandwich or tea bag, the catalyst can be coated directly on the surface of the supported packing as known as the supported catalytic packing. This kind of supported catalytic packing has been proved by some studies [14–

* Corresponding author.
E-mail address: ysha@xmu.edu.cn (Y. Sha).

https://doi.org/10.1016/j.cjche.2022.02.012
1004-9541/

16] to have the lower mass transfer resistance and higher separation efficiency for the CD process, but it still needs to be improved on bonding strength, loading capacity and theoretical investigation [14]. The general acceptability of this supported catalytic packing for the CD system has attracted some attentions recently [16,17]. The strongly coupled reaction–separation interaction resulting from the thin catalyst layer supported on the packing surface also has a lot of academic significance to promote its further understanding and application, and a direct comparison between the supported catalytic packing and tea bag catalytic packing in the same CD process should be useful for this purpose.

In this work, a well-known heterogeneously catalyzed esterification of acetic acid with ethanol is employed to investigate the effect of catalyst loading mode on the CD process. The supported catalytic packing with polystyrene sulfonic acid as the active component was prepared, and its reaction and mass transfer performance were compared with the tea-bag catalytic packing by the lab-scale CD experiment and non-equilibrium stage modeling. For the purpose of deeply understanding to the catalytic packing, by means of the numerical simulation based on the experimental validation, various cases were further designed to investigate the influence of reaction kinetics, mass transfer performance and catalytic efficiency of the supported catalytic packing on CD process.

2. Experimental

2.1. Materials and analysis methods

E44 epoxy oligomer (diglycidyl ether of bisphenol-A (DGEBA) with an epoxide equivalent mass of 210–240 g·equiv^{-1}) and T31 curing agent (phenolic amine curing agent, amine hardener equivalent of 460–480 g·equiv^{-1}) were supplied from Nantong Xingchen Synthetic Material Co., Ltd. (China). Dioctyl phthalate (DOP), acetone, ethanol, poly(4-styrene sulfonic acid) aqueous solution (PSS, $M_w \sim 70000$, 30% (mass)) were used for preparation for the supported catalytic packing, and all of them were supplied from Shanghai Aladdin Biochemical Technology Co., Ltd. (China). The ion exchange resin catalyst Amberlyst 15dry was bought from Rohm and Haas (USA), and packed and sealed by the wire mesh as the teabag catalytic packing (about 15 mm × 8 mm × 40 mm, mass of single package catalyst (0.85 ± 0.15) g, the mesh hole size is 150 μm). The cannon packing (4 mm × 4 mm) was bought from Jiangxi PX Rongjian Environmental Protection Chemical Co., Ltd. (China).

It has been known that there are four components in esterification of acetic acid with ethanol under resin catalysts by GC–MS, and they are acetic acid, ethanol, ethyl acetate and water. Water concentration was analyzed by Karl Fischer titration method, and the rest were analyzed by the gas chromatography (GC9160, Xiamen Jingkejie Intelligent Equipment Co., Ltd., China) with an FID detector and a capillary column (OV-17 with a length of 30 m). The injector and detector temperatures were set to 150 and 230 °C, respectively. The GC column temperature was firstly set to 100 °C for 2 min, then increased at a fixed rate of 30 °C·min^{-1} to 130 °C for 1 min.

2.2. Preparation of supported catalytic packing

The supported catalytic packing was prepared by bonding epoxy porous adhesive layer on the metal canon packing at first, and then loading active components on the adhesive layer. The adhesive solution (mass fraction) consisted of 44% E44, 11% curing agent, 22% DOP and 23% acetone solvent. The dip-coating method was employed for preparing porous layers on metal-based packings. The packings washed by acetone were immersed in the adhesive solution for several minutes, then taken it out and drained off. After repeating the above procedure three times, they were put into the drum dryer for the pre-curing at 70 °C for 2 h and 120 °C for 12 h. The poring agent was eluted by ethanol, and the porous layer can be formed on the surface of the packing. The porous packing was further immersed with diluted 3% (mass) PSS aqueous solution in a vacuum condition to form a thin active layer inside the porous layer, then this active packing was taken into a 90 °C oven for 3 h curing. Finally, the supported catalytic packing can be obtained after 120 °C in oven for a 24 h vacuum drying process. Epoxy particles grafting with PSS, *i.e.* the same catalyst as the supported catalyst on the packing, were prepared in the similar way for the kinetic study of the supported catalyst, and their average particle diameter was screened at about 0.5 mm.

2.3. Kinetics

In order to provide basic kinetic data for the subsequent investigation, the kinetic tests were carried out. The prepared epoxy PSS particles and the commercial Amberlyst 15dry were selected for comparison. A three-neck glass flask fitted with a total reflux condenser to prevent any loss of products was used as a reactor, and it was immersed in a constant temperature bath and provided with a magnetic stirrer. The temperature error range was maintained ±0.5 °C of the set temperature. The equimolar acetic acid and ethanol were preheated respectively to a specified temperature, then were added into the reactor with desired amounts of catalysts. A sufficient stirring speed of 1000 r·min^{-1} was selected to eliminate the external diffusion resistance of heterogeneous catalysts, and this was considered as zero time for the reaction. Considering the formation of azeotropes in the system, the reaction temperature was maintained lower than the lowest azeotropic point at 70.09 °C [18]. Kinetic experiments with different catalysts were conducted at 70 °C, and the influence of the reaction temperature was investigated under 50, 60, and 70 °C. The catalyst concentration was 10.9 g·L^{-1}. During experiments, 0.30 ml samples were withdrawn and analyzed at specified intervals.

2.4. Lab-scale reactive distillation experiments

The lab-scale reactive distillation apparatus (Fig. 1) consists of a column with 1.40 m length and 30 mm internal diameter, the condenser fitted with a relay controller for reflux, a 1000 ml four-neck flask with a stirring heating device as a reboiler. The upper and lower sections of the column are the distillation and stripping sections with the same height of 0.29 m, and the middle section is regarded as the reactive sections with the height of 0.58 m. Two feed ports are located respectively at the top and bottom of the reactive section for acetic acid and ethanol respectively, and there are four temperature sensors and four sampling points along the column. The distillation and stripping sections are loaded with 4 mm × 4 mm cannon packings. For the supported catalytic packings, they are loaded into the whole reactive section. For the teabag catalytic packings (Fig. 2), they are mixed with 4 mm × 4 mm cannon packings in the reactive section for experiments like our previous work [19].

The start-up and shutdown of the CD column are challenging [20–22], so it was carefully proceeded after trial and error. The operating conditions were determined by preliminary tests, then the total feed rate (F) is limited at 15–35 ml·min^{-1}, the reflux ratio (R_r) is at 0.5–3.0, and the distillate flow rate (D) is at 5–15 ml·min^{-1}. All experiments were performed at its steady state which is characterized after the temperature fluctuation of each temperature sensor is under ±1.0 °C [23], and it usually took more than 4 h to reach. The reaction conversion rate (X_i) of the CD process for the reactant is defined as Eq. (1).

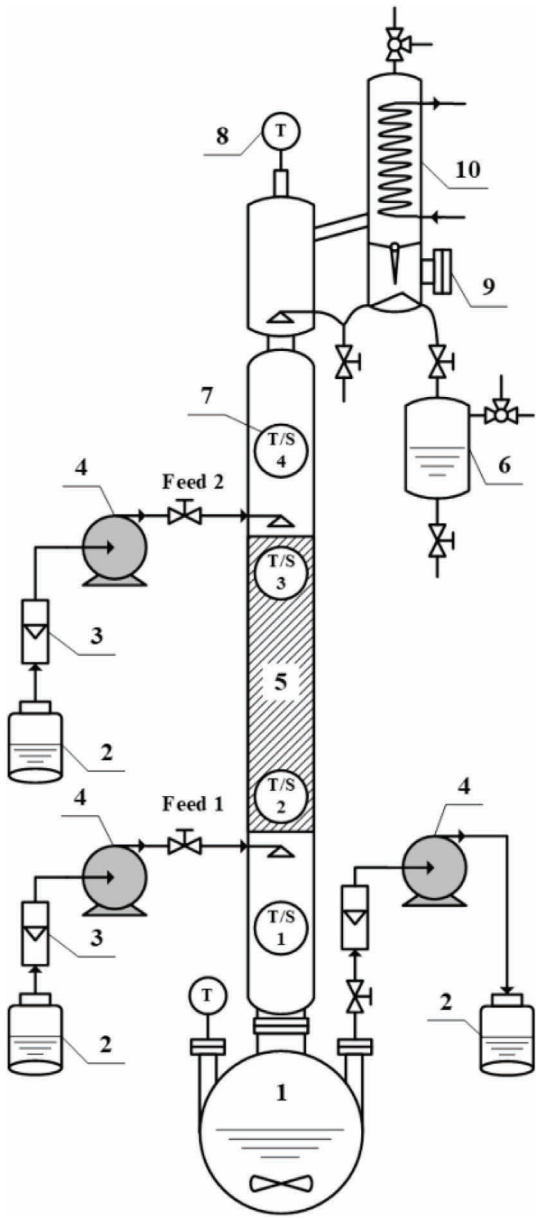

Fig. 1. Sketch of the CD column (1. Reboiler, 2. Storage tank, 3. Rotermeter, 4. Peristaltic pump, 5. Catalytic packings, 6. Receiver tank, 7. Thermometer and sampling point, 8. Thermometer, 9. Magnetic valve, 10. Condenser).

$$X_i = 1 - \frac{Dx_{i,\mathrm{dis}} + Bx_{i,\mathrm{bot}}}{Fx_{i,\mathrm{feed}}} \tag{1}$$

where $x_{i,\mathrm{dis}}$, $x_{i,\mathrm{bot}}$, $x_{i,\mathrm{feed}}$ are the mass fraction of the component i in the liquid phase of the column top distillate, the column bottom discharge and the feed respectively.

3. Results and Discussion

3.1. Characterization of supported catalytic packing

Since PSS is difficult to bond on the metal surface, as mentioned above, firstly, a porous adhesive layer was prepared on the surface, and then the active component, *i.e.* PSS, was deposited in pores by the negative pressure. Thus, the supported catalyst can be prepared. Results from SEM shown as Fig. 2 showed that the supported catalytic packing has a relatively large specific surface area for loading catalyst. The loading amount of the catalyst can be expressed indirectly by the ion exchange capacity (IEC) of catalysts which can be determined by the acid-base titration [14]. Experimental results showed that the IEC of PSS particles was determined at (0.29 ± 0.01) mmol·g^{-1} after repeated tests, and that of the supported catalytic packing based on 4 mm × 4 mm cannon packing was determined at (0.09 ± 0.01) mmol·g^{-1}. The IEC can be maintained at (0.09 ± 0.01) mmol·g^{-1} after the 18 h distillation experiment, and the sulfur content has almost no change by the energy spectrum analysis. It ensured the reliability of subsequent experiments.

3.2. Kinetic model and parameters

The catalytic performance and kinetic equation of PSS and Amberlyst 15dry were studied in order to provide a basis for subsequent CD experiments and process simulation. The effects of catalysts and reaction temperatures on the esterification were investigated by kinetic studies. Fig. 3(a) indicates that the reaction rate using PSS particles is higher than Amberlyst 15dry at the beginning of the reaction. However, its equilibrium conversion rate is similar to that of Amberlyst 15dry.

The reaction system of acetic acid and ethanol is a strong non-ideal system. Non-random two-liquid (NRTL) thermodynamic model was adopted in this work to calculate the vapor–liquid phase equilibrium, and its binary interaction parameters can be found from the literature [24]. The reaction rate (r_i) is described by the quasi-homogeneous model using activity, and it is expressed as Eq. (2). The kinetic constants at different temperatures can be obtained through experimental data in Fig. 3(b). Its details can be found in Supplementary Material as Fig. S1. As a result, the pre-exponential factor is $k_f = 3.805 \times 10^5 \exp(-49355.2/RT)$, kmol·kg^{-1}·s^{-1}, and the chemical equilibrium constant is $\ln(K_{eq}) = 1125.69/T - 0.8521$. The kinetic constants of this esterification using Amberlyst 15dry resin catalyst can be cited from literatures [24,25] for the following process simulation.

$$r_i = m_{\mathrm{cat}}\left(k_f \alpha_{\mathrm{EtOH}} \alpha_{\mathrm{HAc}} - \frac{\alpha_{\mathrm{EtAc}} \alpha_{\mathrm{H_2O}}}{K_{\mathrm{eq}}}\right) \tag{2}$$

where m_{cat} is the mass of catalyst, α_i is the activity of the component i and K_{eq} is the chemical reaction equilibrium constant.

3.3. Results of reactive distillation tests

A reactive section with the 0.58 m height needs 12–15 catalytic teabags mixing with random cannon packings. In this case, the catalyst loaded for the tea-bag catalytic packing in the CD column can reach up to as much as 15.0 g while the supported catalytic packing only has about 1.5 g active catalyst coated on the packing surface. Through the preliminary process simulation, the conversion can be remained almost unchanged when the amount of catalyst was greater than 10.0 g. Therefore, the total 10.23 g catalysts in the whole reactive section was loaded for the tea-bag catalytic packing experiment. Six representative experiments and their results were shown in the Table 1.

Results from the CD experiments show that the process conversion rate using the supported catalytic packing are much higher than that using the tea-bag catalytic packing under the same operating condition, and the dramatic improvement can be up by about 30%. Actually, through the change of feed flow rate (F), molar reflux ratio (R_r) and distillate flow rate (D) from the condenser, some other experiments were also carried out, and they also show the big difference in the conversion rate. The big difference in the conversion rate caused by two catalyst configures in the column may

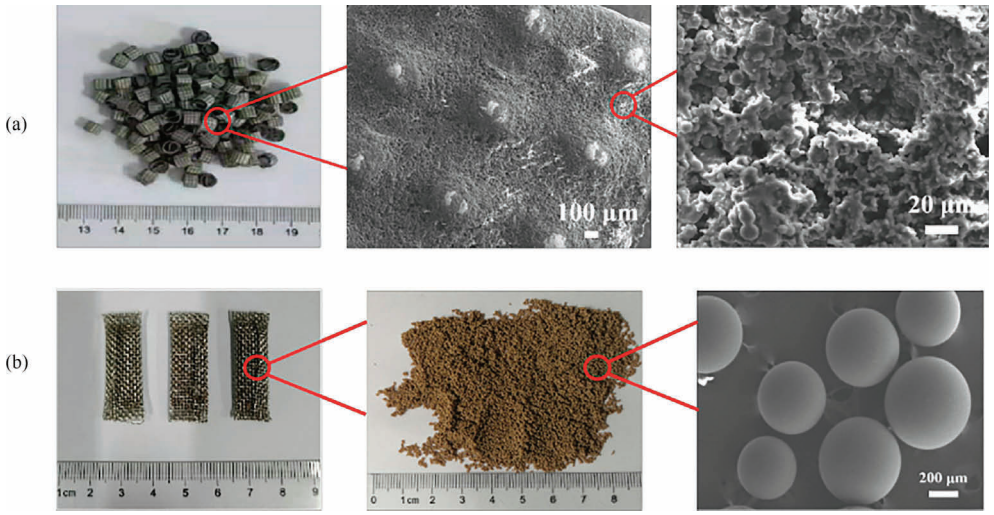

Fig. 2. Catalytic packings in this work: (a) supported catalytic packing, (b) tea-bag catalytic packing.

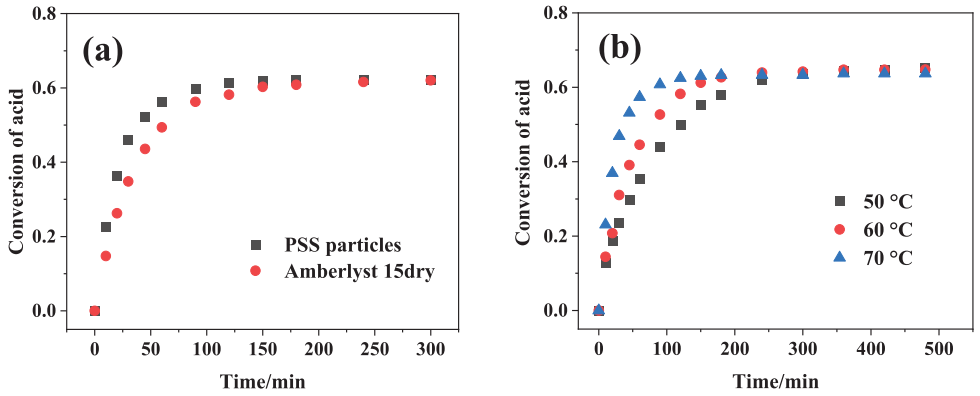

Fig. 3. Effects of (a) catalyst types and (b) reaction temperature on acid conversion.

be attributed to the differences of reaction kinetics, the higher efficiency factor and the good mass transfer performance of the supported catalyst packing. In the kinetic experiment, the supported catalyst showed a significantly high conversion rate in the early stage of the reaction. At the same time, a lot of literatures [14,16,26] have reported that the thin catalyst layer has a higher efficiency factor in the column than the bundle. The higher mass transfer coefficient of the supported catalytic packing is also beneficial to the rapid separation of components and acceleration of the reaction. In an actual process, the above promotion may be synergistic, and it could result in a big difference in the conversion rate. However, it is very difficult to differentiate the specific reason through experiments. For example, it is hardly to prepare the supported catalytic packing and the tea-bag catalytic packing with the same catalytic kinetics, so it is almost impossible to carry out the experiment at the standard with the same reaction base. It is also hardly to conduct experiments with the completely same separation base due to the big difference of the separation performance between the supported catalytic packing and the tea-bag catalytic packing. Hence, the reason for the significant enhancement of the conversion rate is investigated by means of the process simulation which is based on experimental results.

4. Process Simulation and Analysis

4.1. Process approach

The main numerical approach is shown in Fig. 4. The equilibrium model (EQ) is used to set up the preliminary process for the

Table 1
Operation and process conversion of the CD process

NO.	Packings	Mass/g	F_{HAc}; F_{EtOH}/ml·min^{-1}	R_r	D/ml·min^{-1}	X_{HAc}	X_{EtOH}
E1	TBP-15dry①	10.23	10.0; 10.0	1.5	10.0	0.1335	0.1371
E2	TBP-15dry	10.23	10.0; 10.0	1.0	10.0	0.1301	0.1342
E3	TBP-15dry	10.23	10.0; 10.0	0.5	10.0	0.1160	0.1197
E4	SCP-PSS②	1.10	10.0; 10.0	1.5	10.0	0.4302	0.4332
E5	SCP-PSS	1.10	10.0; 10.0	1.0	10.0	0.4289	0.4425
E6	SCP-PSS	1.10	10.0; 10.0	0.5	10.0	0.3508	0.3620

① Tea bag packing filled with Amberlyst 15dry.
② Supported catalytic packing coated with PSS.

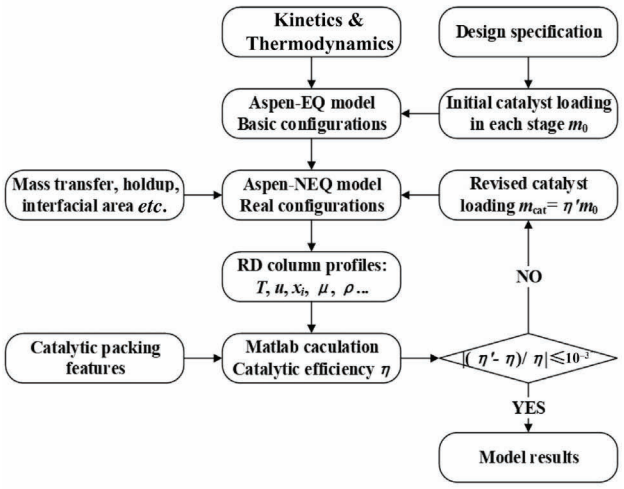

Fig. 4. Scheme for CD process simulation concerning mass transfer.

non-equilibrium stage model (NEQ). The catalytic efficiency is utilized as the convergence criteria to describe the actual catalytic capacity in the process. It can be quantitatively characterized by the efficiency factor. By means of combining the packing features and results from NEQ simulation, the catalytic efficiency was calculated by Matlab software, and combined with kinetic equations as the user subroutine so as to be linked into Aspen software dynamically. The detailed descriptions for this procedure can be found in our previous work [27].

4.2. Process establishment and validation

The total packing height of the experiment column is 1.16 m and selected as the packing height in the process simulation. The equivalent theoretical plate height (H_{ETP}) of 4 mm × 4 mm cannon packings and supported catalytic packings is set to 1/15 m provided by the supplier. Since the reactive section is filled with both the cannon packings and tea-bag catalytic packings in the case of the tea-bag catalytic distillation, the stage number should be modified. Its H_{ETP} is set to 1/5 m according to the structured catalytic packing Katapak-SP [28]. Considering the axial backmixing, the number of packing segments in the NEQ modeling is taken on the base of H_{ETP}/4 for one segment [29], and detailed configurations are listed in Table 2.

In the NEQ model, appropriate correlations should be selected in the process simulation for the better calculation accuracy. Wu *et al.* [30] summarized the correlations of the mass transfer and the interfacial area for catalytic bales packing, so their correlation was selected to describe the mass transfer performance of the tea-bag catalytic packings. Meanwhile, the supported catalytic packing has a similar dimension to the conventional packing, so correlations used for conventional packings were applied to the supported catalytic packing directly. The Onda model [31] was selected to describe the mass transfer of the supported catalytic packing. The work of Billet *et al.* [32] is utilized to calculate the holdup. The Tsai model [33] is used to describe the interfacial areas of packings.

In details, the efficiency factor includes internal and external mass transfer resistances. The efficiency factor for the catalytic packing can be obtained in the form as Eq. (3), and the information of the catalytic packing can be found in Table S1.

$$\eta_{cat} = \frac{D_{e,i}A_{cat}(dc_i/dr)_{r=d_{cat}/2}}{m_{cat}r_{i,b}(T_b, x_{i,b})} \tag{3a}$$

$$\eta_{in} = \frac{D_{e,i}A_{cat}(dc_i/dr)_{r=d_{cat}/2}}{m_{cat}r_{i,s}(T_s, x_{i,s})} \tag{3b}$$

$$\eta_{out} = \frac{r_{i,s}(T_s, x_{i,s})}{r_{i,b}(T_b, x_{i,b})} \tag{3c}$$

where subscripts b and s represent the body and catalyst surface, $D_{e,i}$ is the component i effective diffusion coefficient.

To calculate the efficiency factor, the concentration gradient has to be known in advance. The calculation process of the concentration gradient is as follows. In the reactive section of the CD column, mass and energy conversions for the catalyst can be described as Eqs. (4)–(7) [27].

$$\frac{D_{e,i}}{r^m}\frac{d}{dr}\left(r^m\frac{dc_i}{dr}\right) + \upsilon_i\rho_{cat}r_i = 0 \tag{4}$$

$$\frac{\lambda_{cat}}{r^m}\frac{d}{dr}\left(r^m\frac{dT}{dr}\right) + \sum\rho_{cat}r_i(-\Delta Hr_i) = 0 \tag{5}$$

Its boundary conditions are shown as below.

$$r = 0,\ \frac{dc_i}{dr} = \frac{dT}{dr} = 0 \tag{6}$$

$$r = \frac{d_{cat}}{2},\ D_{e,i}\frac{dc_i}{dr} = k_{s,i}(c_{i,b} - c_i);\ \lambda_{cat}\frac{dT}{dr} = h_s(T_b - T_s) \tag{7}$$

In the case of the particle catalyst, the value of the exponential term m is 2, and it is adopted for tea-bag catalytic packing. For the plate catalyst, m is 0 [27], and it is adopted for supported catalytic packing. The diffusion coefficient ($D_{i,m}$) in the liquid phase was calculated by the Wilke–Change equation [34], and the effective diffusion coefficient ($D_{e,i}$) inside of catalysts was modified as $D_{e,i} = D_{i,m}\cdot\varepsilon_{cat}/\tau_{cat}$. The Chilton–Colburn analogy was used to calculate the mass and heat transfer coefficients between the liquid phase and the solid phase [35,36] as Eq. (8).

$$\frac{k_s}{u_L}Sc^{2/3} = \frac{h_s}{c_p u_L}Pr^{2/3} = \frac{0.765}{Re^{0.82}} + \frac{0.365}{Re^{0.386}} \tag{8}$$

where $Sc = \mu/\rho D$, $Pr = c_p\cdot\mu_L/\lambda_L$, $Re = d_{cat}\cdot\rho\cdot u_L/\mu_L\varepsilon_{cat}$.

It should be noted that the liquid velocity u_L inside and outside the catalyst bag is classified by an distribute coefficient γ [5,8,37].

Table 2
Column configurations in models for process simulation

Location①	H_p②/m	EQ		NEQ	
		N_{SCP}③	N_{TBP}③	N_{SCP}③	N_{TBP}③
Distillation section	0.29	4	4	16	16
Reaction section	0.58	9	3	37	13
Stripping section	0.29	4	4	16	16
Reboiler	–	1	1	1	1

① The label can refer to Fig. 1.
② Packing height.
③ For EQ, N represents the number of theoretical plates; For NEQ, N represents the number of segments in the NEQ model.

So far, the concentration gradient dc_i/dr can be solved through mass, energy equations combining boundary conditions as shown above, and the efficiency factor can be acquired. Other detailed descriptions for calculation of the efficiency factor can also be found in our previous work [27].

The established EQ and NEQ models were verified by means of results from experiments in Section 3.3. Results from E2 using tea-bag catalytic packings and E5 using supported catalytic packings are shown as examples in Fig. 5, and the experimental information for E2 and E5 can be found in Table 1.

Results from the NEQ model are more accurate than those from the EQ model, especially for the reactive section with TBP (Fig. 5(a) and (b)). The main reason is that the EQ model does not include the influence of internal hardware of the column, and the different catalytic packings have great influence on the performance of the CD column. Results also indicate that correlations utilized in the process simulation are suitable, and the NEQ model is reliable to describe the CD process with either supported catalytic packings or tea-bag catalytic packings. For the CD process with supported catalytic packings, results from the EQ model is close to results from the NEQ model (Fig. 5(c) and (d)) though the EQ model has a large deviation to predict performance of tea-bag catalytic packings. It implies that the thin catalyst layer on the packing surface has little influence on the mass transfer performance of the packing. In order to ensure reliability of the simulation, the NEQ model is adopted in the following section for investigation by the process simulation.

4.3. Case design

In view of the good agreement between the NEQ model established in this work and the experiment, the big difference between supported catalytic packing and tea-bag catalytic packing can be analyzed by changing corresponding model parameters in the NEQ model, such as kinetics and mass transfer coefficient. Since there is no way to change these parameters as required through experiments, it seems like a convenient method to analyze the performance of the supported catalytic packing.

By replacing the reactive kinetics of the tea-bag catalytic packing with that of the PSS catalyst, it can ensure that the separation performances of the tea-bag catalytic packing with different reactive abilities are same. It is equivalent to replace active ingredients in Amberlyst 15dry with the PSS catalyst while the geometry of Amberlyst 15dry and the catalyst packing keep same. Therefore, influence of the reactive ability on the CD process can be studied by means of virtual cases marked as TBP-PSS. In addition, with different catalyst loading methods, *i.e.* tea-bag catalytic packing and supported catalytic packing, under the condition with the same amount of the same PSS catalyst, influence of the separation ability of different catalyst packings on the CD process can be studied. Case studies were carried out at fixed operating conditions, and results are listed in Table 3.

4.4. Case study

As mentioned in the distillation experiment above, the process simulation also observed that supported catalytic packing can achieve high ethyl acetate conversion rate at a low catalyst loading, and it has a significant difference with TBP-15dry. As shown as C1 *vs.* C2, the process conversion (X_{eff}) can increase from 0.0875 to 0.3714 when Amberlyst 15dry was substituted by PSS in the catalytic packings, and it shows the big contribution of the reaction kinetics to the process of this system. Interestingly, when the tea-bag catalytic packing and the supported catalytic packing are

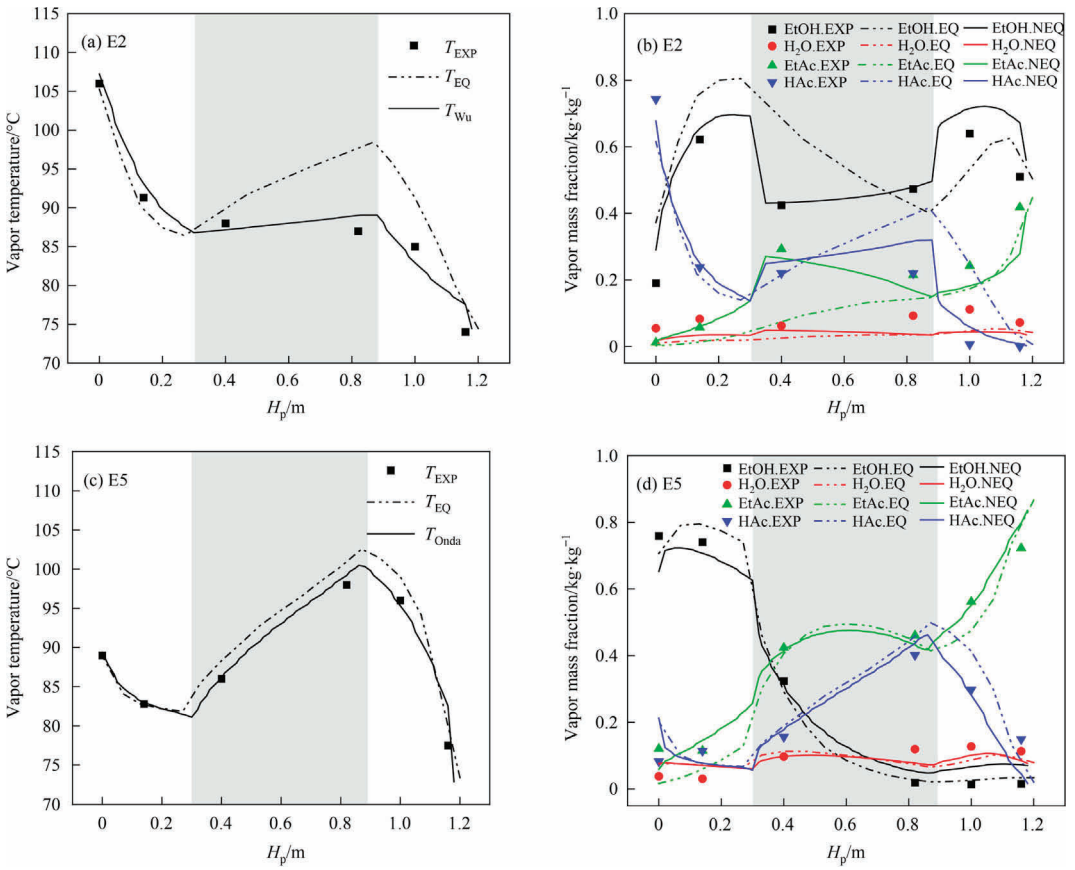

Fig. 5. Model validation: (a, c) temperature and (b, d) composition profiles.

Table 3
Operating condition and process conversion of the CD process

Cases	Packings	Mass/g	F_{HAc}; F_{EtOH}/kmol·h^{-1}	R_r	D/kg·h^{-1}	X_{eff}②
C1	TBP-15dry	10.0①	0.1;0.1	1.0	0.5	0.0875
C2	TBP-PSS(a)	10.0①	0.1;0.1	1.0	0.5	0.3714
C3	TBP-PSS(b)	1.0	0.1;0.1	1.0	0.5	0.2123
C4	SCP-PSS	1.0	0.1;0.1	1.0	0.5	0.3942

① The conversion change little while the loading amount of catalyst is more than 10.0 g.
② Acetic acid and ethanol have the same conversion rate under operating conditions.

at the same PSS loading, as shown as C3 *vs*. C4, the conversion still shows significant difference 0.2123 *vs*. 0.3942. Since the intrinsic reaction kinetics of both the supported catalytic packing and the tea-bag catalytic packing are the same in this situation, this difference can only be attributed to difference of the separation performance between supported catalytic packing and tea-bag catalytic packing, *i.e*. mass transfer-related effects, such as the difference of diffusion or distillation, induced by the different catalyst loading form.

The loading form of the catalyst may cause change of the actual catalyst efficiency, which can be compared by efficiency factor. Sundmacher *et al*. [26] conducted research on the supported catalytic packing, and found that it could have an efficiency factor of almost 1. Since the efficiency factor range of tea-bag catalytic packings is 0.35–0.85 [6], the difference of efficiency factors may be one of reasons for the performance difference between the supported catalytic packing and the tea bag catalytic packing. The efficiency factor includes the internal diffusion efficiency factor and the external diffusion efficiency factor. The internal diffusion efficiency factor is related to the size or thickness of catalyst particles. The thickness of the catalytic layer of SCP-PSS is only about 0.1 mm. According to computational results, the internal catalytic efficiency of the SCP-PSS is about 0.85 on average, and it is higher than 0.65 of TBP-PSS(b) as shown in Fig. 6. This is mainly caused by the different thickness of catalyst. The external diffusion efficiency factor is mainly related to the external flow, and is also affected by the component transfer caused by the vapor–liquid phase separation in catalytic distillation. Different from the internal diffusion, it is relatively easy to improve the external diffusion by means of changing the packing configure and operation, and many progresses have been made in this area. The external efficiency factor for TBP-PSS(b) is only about 0.25 while SCP-PSS can reach about 0.75, and the difference is almost three times. According to experimental results of teabag like catalytic packings [38], the fluid flow on the catalyst particle surface inside the catalyst bag is hindered by packages, and the liquid flow rate on the catalyst surface is about one tenth of that on the package surface. It increases the mass transfer resistance in the liquid phase. In addition, the reaction products accumulate on the surface of the catalyst and further reduce the reaction rate and conversion. For the supported catalytic packing, the catalyst layer is directly exposed in the main body of the vapor–liquid phase, and it has a low mass transfer resistance. It means that the reaction products can be removed in time from the liquid phase to the vapor phase through distillation separation. This "*in-situ* separation" performance of SCP-PSS accelerates the esterification, and can promote the process conversion greatly. This can be proved by the effective equal plate height calculated by the NEQ model. As shown in Fig. 7, the equal plate height of the reaction section for the supported catalytic packing is much lower than that of the tea-bag catalytic packing.

With regard to reaction rates in the tea-bag catalytic packing and the supported catalytic packing along the reaction section, the significantly different reaction rates along the reactive packing height happens as shown as in Fig. 8. Since the reaction rate is related to the component concentration, the composition distribution in the liquid phase along the column is acquired as Fig. 9 for C3 and C4, and it is similar to experimental data (Fig. 5). From the viewpoint of reactants, acetic acid and ethanol have significantly different volatilities. Since acetic acid as the heavy component is

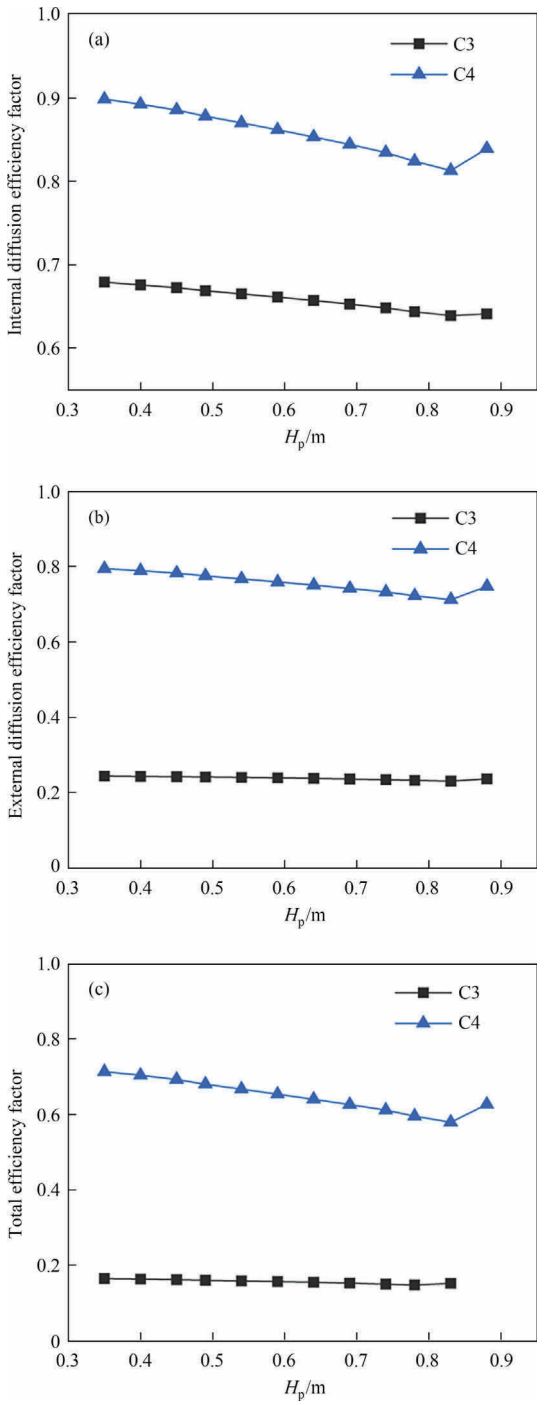

Fig. 6. (a) Internal, (b) external and (c) total efficiency factor in the reactive section.

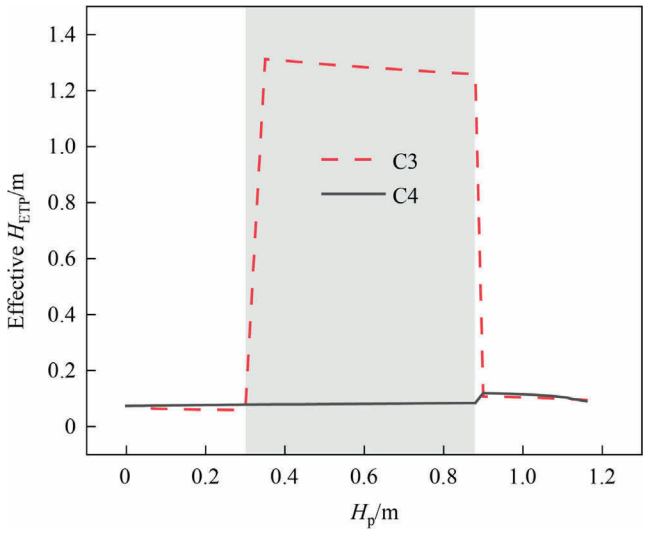

Fig. 7. Effective H_{ETP} of two catalytic packings in the CD column.

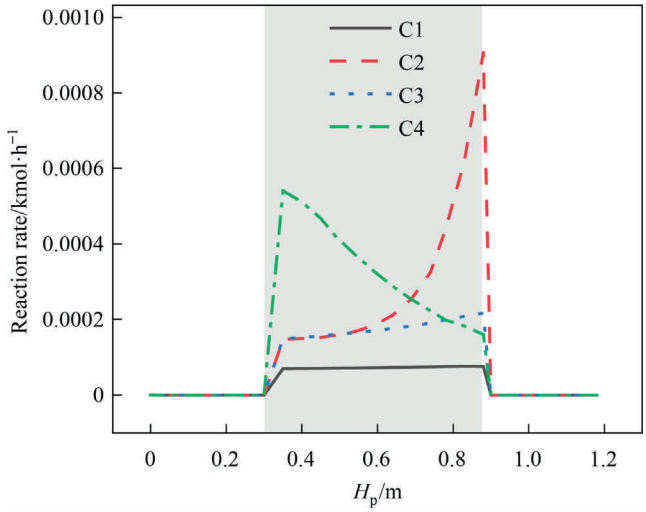

Fig. 8. Reaction rates profiles in the CD column using different catalytic packings (based on the formation rate of ethyl acetate).

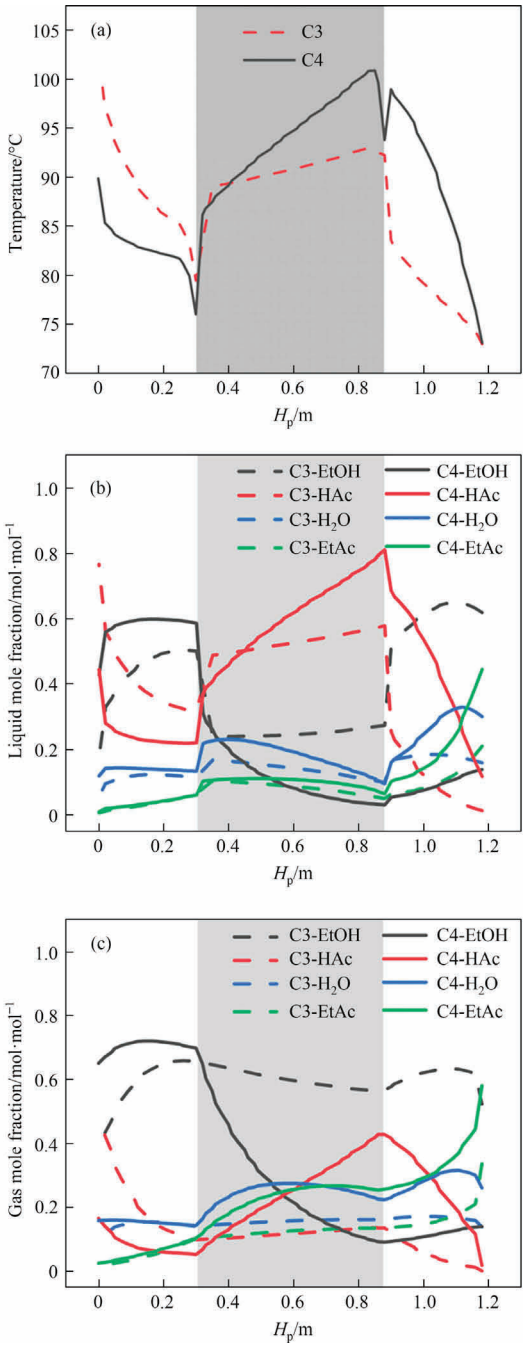

Fig. 9. Temperature (a), liquid composition (b) and vapor composition (c) profiles in CD column.

fed from the top of the reaction section, its concentration along the downward liquid phase is always high. However, ethanol is fed from the bottom of the reaction section, its concentration in the liquid phase of the reaction section depends on the vapor–liquid mass transfer in the distillation. Due to the better mass transfer performance of the supported catalytic packing, ethanol, which can be considered as the light component in this esterification system, its concentration in the liquid phase of the upper reaction section is very low while its concentration in the lower reaction section is high. Thus the high reaction rate locates in the lower reaction section. For the tea-bag catalytic packing, it has a relatively weak vapor–liquid separation performance. The concentration of ethyl acetate produced by esterification increases along the downward liquid phase because ethyl acetate cannot be separated from the liquid phase to the vapor phase quickly. Enrichment of ethyl acetate along the downward liquid phase limits the reaction rate, so the high reaction rate locates in the upper reaction section for the tea-bag catalytic packing. Meanwhile, as shown in Fig. 9(a), the temperature of the reaction section loaded by the tea-bag catalytic packing is lower than that loaded by the supported catalytic packing because there are more light components in the liquid phase in the case of the tea-bag catalytic packing. Due to the relatively weak vapor–liquid separation performance of the tea-bag catalytic packing, even if the reaction activity is very good, it is difficult to improve the reaction rate due to accumulation of ethyl acetate in the liquid phase (Fig. 9(b)). This illustrates the coupled effect between reaction and separation.

In general, the synergism of catalyst kinetics, efficiency factor and mass transfer performance leads to significant differences in the performance of the supported catalytic packing and the tea-bag catalytic packing. Although the catalyst loading amount of

the supported catalytic packing is limited, the experiment and the numerical simulation shows advantages of the surface supported catalyst with high activity and high separation performance. The rapid "*in-situ* separation" caused by the high mass transfer performance of the supported catalytic packing can significantly improve the reaction conversion under a low load amount. With the consideration of some recent progresses in the material preparation and the high-efficiency catalyst, some restrictions for the supported catalytic packing could be resolved for the better bonding strength between catalyst and surface, the bigger specific surface area and the higher catalytic activity [39,40], and it should be helpful for its application.

5. Conclusions

In this work, for the esterification CD of acetic acid with ethanol, by comparing the CD performance of the supported catalytic packing and the tea-bag catalytic packing through the experiment and the numerical simulation, the following conclusions can be obtained:

(1) The supported catalytic packing can significantly improve the reaction conversion under a one tenth loading amount in comparison with the tea-bag catalytic packing. It can be attributed to its relatively better reaction kinetics and mass transfer performance.
(2) The established NEQ model including the catalyst efficiency can be utilized to predict the CD process with both the tea-bag catalytic packing and the supported catalytic packing. The EQ model can be utilized to predict the CD process with the supported catalytic packing because the thin catalyst layer has little influence on the mass transfer performance of the packing.
(3) For the tea-bag catalytic packing, the kinetics of the catalyst has a significant influence on the conversion rate of the CD process, and it suggests that a highly efficient catalyst can significantly improve the original CD process as shown as C1 and C2 in Table 3. The tea-bag catalytic packing has a low efficiency factor and a poor mass transfer performance when the reaction kinetics of PSS is used, and these can result in a low conversion rate.
(4) Due to the better separation performance, distributions of the reaction rate, temperature and composition with the supported catalytic packing in the column are different from that with the tea-bag catalytic packing. The high reaction rate locates in the upper reaction section loaded by the tea-bag catalytic packing while it locates in the lower reaction section loaded by the supported catalytic packing. It can be attributed to different distributions of the reactant and product due to different separation abilities. Quantitative results from this work should be beneficial for its further development.

CRediT Authorship Contribution Statement

Zhiwei Wang: Writing – original draft, Data curation, Investigation, Conceptualization. **Yu Zhang:** Visualization. **Zhi Zhang:** Visualization. **Daowei Zhou:** Writing – review & editing. **Zhikai Cao:** Writing – review & editing. **Yong Sha:** Methodology, Conceptualization, Supervision.

Data Availability

The data that has been used is confidential.

Declaration of Competing Interest

The authors declare that they have no known competing financial interests or personal relationships that could have appeared to influence the work reported in this paper.

Acknowledgements

The authors acknowledge financial support provided by National Natural Science Foundation of China (21978243).

Supplementary Material

Supplementary data to this article can be found online at https://doi.org/10.1016/j.cjche.2022.02.012.

Nomenclature

A	surface area, m^2
B	liquid flow rate at the bottom of column, $ml \cdot min^{-1}$
c	molar concentration, $kmol \cdot m^{-3}$
D	distillate flow rate, $ml \cdot min^{-1}$
D_e	diffusion coefficient inside of catalysts, $m^2 \cdot s^{-1}$
D_m	diffusion coefficient in the liquid phase
d	diameter, m
F	feed flow rate, $ml \cdot min^{-1}$
h_s	heat transfer coefficient, $W \cdot m^{-2} \cdot K^{-1}$
K_{eq}	chemical reaction equilibrium constant
k_f	pre-exponential factor, $kmol \cdot kg^{-1} \cdot s^{-1}$
m_{cat}	mass of catalyst, kg
m	exponential term
Pr	Prandtl number
Re	Reynold number
R_r	reflux ratio
r	reaction rate
Sc	Schmidt number
T	temperature, K
u_L	liquid velocity, $m \cdot s^{-1}$
X	reaction conversion rate
α	activity
γ	distribute coefficient
ε	porosity
η	effectiveness factor
λ	thermal conductivity, $W \cdot m^{-1} \cdot K^{-1}$
ρ	density, $kg \cdot m^{-3}$
τ	tortuosity factor
μ_L	viscosity of liquid, Pa·s
v	stoichiometric coefficient

Subscripts

b	body surface
cat	catalyst
i	component i
in	internal diffusion
out	external diffusion
s	catalyst surface

References

[1] A.A. Kiss, M. Jobson, X. Gao, Reactive distillation: Stepping up to the next level of process intensification, *Ind. Eng. Chem. Res.* 58 (15) (2019) 5909–5918.
[2] J.J. Liu, B.L. Yang, Liquid–liquid–solid mass transfer and phase behavior of heterogeneous etherification of glycerol with isobutene, *AIChE J.* 64 (7) (2018) 2526–2535.
[3] P.W.A.M. Wenmakers, J. van der Schaaf, B.F.M. Kuster, J.C. Schouten, Liquid–solid mass transfer for cocurrent gas–liquid upflow through solid foam

packings, *AIChE J.* 56 (11) (2010) 2923–2933.
[4] N. Bekiaris, G.A. Meski, C.M. Radu, M. Morari, Multiple steady states in homogeneous azeotropic distillation, *Ind. Eng. Chem. Res.* 32 (9) (1993) 2023–2038.
[5] K. Sundmacher, G. Uhde, U. Hoffmann, Multiple reactions in catalytic distillation processes for the production of the fuel oxygenates MTBE and TAME: Analysis by rigorous model and experimental validation, *Chem. Eng. Sci.* 54 (13–14) (1999) 2839–2847.
[6] Q.L. Wang, C. Yang, H.X. Wang, T. Qiu, Optimization of process-specific catalytic packing in catalytic distillation process: A multi-scale strategy, *Chem. Eng. Sci.* 174 (2017) 472–486.
[7] X.G. Li, H. Zhang, X. Gao, R. Zhang, H. Li, Hydrodynamic simulations of seepage catalytic packing internal for catalytic distillation column, *Ind. Eng. Chem. Res.* 51 (43) (2012) 14236–14246.
[8] C.N. Dai, Z.G. Lei, Q.S. Li, B.H. Chen, Pressure drop and mass transfer study in structured catalytic packings, *Sep. Purif. Technol.* 98 (2012) 78–87.
[9] H.D. Ding, J.M. Li, W.Y. Xiang, C.J. Liu, CFD simulation and optimization of winpak-based modular catalytic structured packing, *Ind. Eng. Chem. Res.* 54 (8) (2015) 2391–2403.
[10] Q.L. Wang, F.Y. Zhang, R. Huang, X.D. Wang, C. Yang, H.X. Wang, T. Qiu, Multiphase flow and multicomponent reactive transport study in the catalyst layer of structured catalytic packings for the direct hydration of cyclohexene, *Chem. Eng. Process. Process. Intensif.* 158 (2020) 108199.
[11] L. Götze, O. Bailer, P. Moritz, C. von Scala, Reactive distillation with KATAPAK®, *Catal. Today* 69 (1–4) (2001) 201–208.
[12] X. Gao, F.Z. Wang, R. Zhang, H. Li, X.G. Li, Liquid flow behavior of a seepage catalytic packing internal for catalytic distillation column, *Ind. Eng. Chem. Res.* 53 (32) (2014) 12793–12801.
[13] X. Gao, Q.Y. Ding, Y. Wu, Y.L. Jiao, J.S. Zhang, X.G. Li, H. Li, Kinetic study of esterification over structured ZSM-5-coated catalysts based on fluid flow situations in macrocellular foam materials, *React. Chem. Eng.* 5 (3) (2020) 485–494.
[14] T. Deng, Y.K. Li, G.F. Zhao, Z.Q. Zhang, Y. Liu, Y. Lu, Catalytic distillation for ethyl acetate synthesis using microfibrous-structured Nafion–SiO_2/SS-fiber solid acid packings, *React. Chem. Eng.* 1 (4) (2016) 409–417.
[15] K. Sundmacher, U. Hoffmann, Multicomponent mass and energy transport on different length scales in a packed reactive distillation column for heterogeneously catalysed fuel ether production, *Chem. Eng. Sci.* 49 (24) (1994) 4443–4464.
[16] X. Gao, P. Yan, X.H. Ma, Z.Y. Zhao, H. Li, X.G. Li, Design of distillation reactor with novel catalysts distribution pattern for *n*-amyl acetate synthesis in industrial scale, *Fuel* 280 (2020) 118604.
[17] Y.L. Jiao, C.H. Jiang, Z.M. Yang, J. Liu, J.S. Zhang, Synthesis of highly accessible ZSM-5 coatings on SiC foam support for MTP reaction, *Microporous Mesoporous Mater.* 181 (2013) 201–207.
[18] Y.T. Tang, Y.W. Chen, H.P. Huang, C.C. Yu, S.B. Hung, M.J. Lee, Design of reactive distillations for acetic acid esterification, *AIChE J.* 51 (6) (2005) 1683–1699.
[19] J.C. Ye, J. Li, Y. Sha, Y.L. Xu, D.W. Zhou, Novel reactive distillation process for phenol production with a dry cation exchange resin as the catalyst, *Ind. Eng. Chem. Res.* 53 (32) (2014) 12614–12621.
[20] F. Reepmeyer, J.U. Repke, G. Wozny, Time optimal start-up strategies for reactive distillation columns, *Chem. Eng. Sci.* 59 (20) (2004) 4339–4347.
[21] H.X. Wu, Z.G. Tang, H. Hu, C. Quan, H.H. Song, S.Y. Li, Predictions for start-up processes of reactive distillation column *via* artificial neural network, *Chem. Eng. Technol.* 29 (6) (2006) 744–749.
[22] R.L.N. de la Fuente, A.F. Tlacuahuac, Optimal start-up and product transition policies of a reactive distillation column, *Ind. Eng. Chem. Res.* 46 (7) (2007) 2092–2111.
[23] T. Keller, J. Muendges, A. Jantharasuk, C.A. Gónzalez-Rugerio, H. Moritz, P. Kreis, A. Górak, Experimental model validation for *n*-propyl propionate synthesis in a reactive distillation column coupled with a liquid–liquid phase separator, *Chem. Eng. Sci.* 66 (20) (2011) 4889–4900.
[24] N. Calvar, B. González, A. Dominguez, Esterification of acetic acid with ethanol: Reaction kinetics and operation in a packed bed reactive distillation column, *Chem. Eng. Process. Process. Intensif.* 46 (12) (2007) 1317–1323.
[25] I.K. Lai, Y.C. Liu, C.C. Yu, M.J. Lee, H.P. Huang, Production of high-purity ethyl acetate using reactive distillation: Experimental and start-up procedure, *Chem. Eng. Process. Process. Intensif.* 47 (9–10) (2008) 1831–1843.
[26] K. Sundmacher, H. Künne, U. Kunz, Contribution of gel phase diffusion to mass transfer in supported ion exchange catalysts, *Chem. Eng. Technol.* 21 (6) (1998) 494–498.
[27] Y.Y. Zhuo, Y.X. Zhong, Y.L. Xu, Y. Sha, Evaluation of transfer resistances in the reactive distillation process for phenol production, *Ind. Eng. Chem. Res.* 55 (1) (2016) 257–266.
[28] P. Moritz, H. Hasse, Fluid dynamics in reactive distillation packing Katapak®-S, *Chem. Eng. Sci.* 54 (10) (1999) 1367–1374.
[29] Z. Fan, K. Liu, G.J. Qi, R. Frimpong, H. Nikolic, K.L. Liu, Aspen modeling for MEA–CO_2 loop: Dynamic gridding for accurate column profile, *Int. J. Greenh. Gas Control* 37 (2015) 318–324.
[30] Y. Wu, Study of catalytic distillation hydrolysis of methyl acetate in a pilot plant, Ph. D. Thesis, Zhejiang Univ, China, 1999.
[31] K. Onda, H. Takeuchi, Y. Okumoto, Mass transfer coefficients between gas and liquid phases in packed columns, *J. Chem. Eng. Jpn.* 1 (1) (1968) 56–62.
[32] R. Billet, M. Schultes, Prediction of mass transfer columns with dumped and arranged packings: Updated summary of the calculation method of Billet and Schultes, *Chem. Eng. Res. Des.* 77 (6) (1999) 498–504.
[33] R.E. Tsai, A.F. Seibert, R.B. Eldridge, G.T. Rochelle, A dimensionless model for predicting the mass-transfer area of structured packing, *AIChE J.* 57 (5) (2011) 1173–1184.
[34] C.R. Wilke, P. Chang, Correlation of diffusion coefficients in dilute solutions, *AIChE J.* 1 (2) (1955) 264–270.
[35] T.H. Chilton, A.P. Colburn, Mass transfer (absorption) coefficients prediction from data on heat transfer and fluid friction, *Ind. Eng. Chem.* 26 (11) (1934) 1183–1187.
[36] P.N. Dwivedi, S.N. Upadhyay, Particle-fluid mass transfer in fixed and fluidized beds, *Ind. Eng. Chem. Proc. Des. Dev.* 16 (2) (1977) 157–165.
[37] A. Hoffmann, C. Noeres, A. Górak, Scale-up of reactive distillation columns with catalytic packings, *Chem. Eng. Process. Process. Intensif.* 43 (3) (2004) 383–395.
[38] S. Ratheesh, A. Kannan, Holdup and pressure drop studies in structured packings with catalysts, *Chem. Eng. J.* 104 (1–3) (2004) 45–54.
[39] T. Deng, J. Ding, G.F. Zhao, Y. Liu, Y. Lu, Catalytic distillation for esterification of acetic acid with ethanol: Promising SS-fiber@HZSM-5 catalytic packings and experimental optimization via response surface methodology, *J. Chem. Technol. Biotechnol.* 93 (3) (2018) 827–841.
[40] T. Deng, G.F. Zhao, Y. Liu, Y. Lu, Catalytic distillation for one-step cyclohexyl acetate production and cyclohexene-cyclohexane separation via esterification of cyclohexene with acetic acid over microfibrous-structured Nafion-SiO_2/SS-fiber packings, *Chem. Eng. Process. Process. Intensif.* 131 (2018) 215–226.